Cardiovascular Research (2011) **90**, 546–556
doi:10.1093/cvr/cvr018

Placental stem cells pre-treated with a hyaluronan mixed ester of butyric and retinoic acid to cure infarcted pig hearts: a multimodal study

Anca Simioniuc[1], Manuela Campan[1], Vincenzo Lionetti[1,2], Martina Marinelli[1], Giovanni D. Aquaro[2], Claudia Cavallini[3], Sabrina Valente[4], Dario Di Silvestre[5], Silvia Cantoni[3], Fabio Bernini[1], Claudia Simi[1,6], Silvia Pardini[6], Pierluigi Mauri[5], Danilo Neglia[2], Carlo Ventura[3], Gianandrea Pasquinelli[4], and Fabio A. Recchia[1,2,7]*

[1]Guppo Intini-SMA Laboratory of Experimental Cardiology, Scuola Superiore Sant'Anna, I-56124 Pisa, Italy; [2]Fondazione CNR-Regione Toscana "G. Monasterio", I-56124 Pisa, Italy; [3]Laboratory of Molecular Biology and Stem Cell Engineering, Department of Cardiology, National Institute of Biostructures and Biosystems, University of Bologna, I-40138 Bologna, Italy; [4]Department of Hematology, Oncology and Clinical Pathology, University of Bologna, I-40138 Bologna, Italy; [5]Institute for Biomedical Technologies, Proteomics and Metabolomics Unit - CNR, I-20090 Segrate, Milan, Italy; [6]Department of PET and Radiopharmaceutical Chemistry, Institute of Clinical Physiology, CNR, Pisa, Italy; and [7]Department of Physiology, New York Medical College, Valhalla, NY 10595, USA

Received 6 October 2010; revised 11 January 2011; accepted 13 January 2011; online publish-ahead-of-print 21 January 2011

Time for primary review: 22 days

Aims Pre-treating placenta-derived human mesenchymal stem cells (FMhMSCs) with a hyaluronan mixed ester of butyric and retinoic acid (HBR) potentiates their reparative capacity in rodent hearts. Our aim was to test FMhMSCs in a large-animal model by employing a novel combination of *in vivo* and *ex vivo* analyses.

Methods and results Matched regional quantifications of myocardial function and viability were performed by magnetic resonance imaging (MRI) and positron emission tomography (PET) 4 weeks after myocardial infarction combined with intramyocardial injection of FMhMSCs ($n = 7$), or HBR-pre-treated FMhMSCs (HBR-FMhMSCs, $n = 6$), or saline solution (PBS, $n = 7$). Sham-operated pigs ($n = 4$) were used as control animals. Despite no differences in the ejection fraction and haemodynamics, regional MRI revealed, in pigs treated with HBR-FMhMSCs compared with the other infarcted groups, a 40% smaller infarct scar size and a significant improvement of the end-systolic wall thickening and circumferential shortening of the infarct border zone. Consistently, PET showed that myocardial perfusion and glucose uptake were, respectively, 35 and 23% higher in the border zone of pigs treated with HBR-FMhMSCs compared with the other infarcted groups. Histology supported *in vivo* imaging; the delivery of HBR-FMhMSCs significantly enhanced capillary density and decreased fibrous tissue by approximately 68%. Moreover, proteomic analysis of the border zone in the HBR-FMhMSCs group and the FMhMSCs group indicated, respectively, 45 and 30% phenotypic homology with healthy tissue, while this homology was only 26% in the border zone of the PBS group.

Conclusion Our results support a more pronounced reparative potential of HBR-pre-treated FMhMSCs in a clinically relevant animal model of infarction and highlight the necessity of using combined diagnostic imaging to avoid underestimations of stem cell therapeutic effects in the heart.

Keywords Myocardial infarction • Stem cells • Positron emission tomography • Magnetic resonance imaging • Proteome

1. Introduction

Once a candidate stem cell type for cardiac regeneration has been successfully tested in rodents, the subsequent recommendable step, albeit sometimes neglected, before the experimental findings are translated into clinical medicine, is to validate the new therapy in large-animal model. This process implies scaling up cell delivery, which might prove difficult and reveal previous overestimations of

* Corresponding author: Sector of Medicine, Scuola Superiore Sant'Anna, Piazza Martiri della Libertà, 33-56127 Pisa, Italy. Tel: +39 050 3152216, Fax: +39 050 3152166, Email: f.recchia@sssup.it, fabio_recchia@nymc.edu

the beneficial effects. In addition, large mammals allow much finer assessments of cardiac function with standard diagnostic imaging and therefore more reliable and clinically relevant estimations of the reparative capacity of stem cells.

We have previously tested, in a rat model of myocardial infarction (MI), the cardio-regenerative properties of human mesenchymal stem cells obtained from term placenta and pre-conditioned *in vitro* with a mixed ester of hyaluronan, butyric, and retinoic acid (HBR).[1] Placental stem cells are emerging as appealing candidates for regenerative therapy,[2,3] in that they can be harvested in large quantities, stored at birth for later use, and easily expanded, and are characterized by prominent multi-potency and low immunogenicity.[3,4] We found that, after direct intra-myocardial injection in the border zone, HBR-pre-conditioned mesenchymal cells differentiated as vascular and muscle tissue and caused a marked reduction in infarct size.[1] Also, stem cells not pre-treated with HBR, although unable to regenerate cardiac tissue directly, caused a significant, but more modest reduction in infarct size. The only assessment of cardiac function was based on ejection fraction; hence, we could not determine possible correlations between different histological patterns of tissue regeneration and contractile performance and metabolism at the sites of cell implantation. Given these premises, the aim of the present study was to test the effects of implantation of human placental stem cells in a large-animal model of myocardial infarction; a particular focus was put on regional function and metabolism, since cell therapy of myocardial infarction targets primarily certain regions of the heart. To pursue our objective, we used a combination of positron emission tomography (PET) and magnetic resonance imaging (MRI), which are the gold standard for *in vivo* quantitative assessment of, respectively, myocardial flow/metabolism and contractile performance in well-defined segments of the cardiac wall.[5,6] Moreover, MRI allows an accurate determination of infarct size in the beating heart.[7,8] *In vivo* data were then corroborated by proteomic and histological analysis. The availability of selective anti-human antibodies enabled us to identify implanted cells and track their differentiation in the host pig tissue.

2. Methods

2.1 Synthesis of HBR

The glycoconjugate HBR is an ester between the hydroxyl groups of hyaluronan and the carboxyl groups of butyric acid and retinoic acid. The procedure for HBR synthesis and characterization is presented in detail elsewhere (see Supplementary material online).[9]

2.2 Mesenchymal stem cell isolation and culture

Fetal membrane-derived human mesenchymal stem cells (FMhMSCs) were isolated as previously described.[1] FMhMSCs were cultured for 14 days without or with 1.5 mg/mL HBR in culture medium (HBR-FMhMSCs).[1] Our investigation conformed with the principles outlined in the Declaration of Helsinki. According to the policy approved by our local ethical committee at the S. Orsola-Malpighi Hospital of the University of Bologna, Italy, all tissue samples were obtained after informed consent.

2.3 Myocardial infarction and stem cell transplantation

Thirty-two male, castrated farm pigs (35–40 kg) were sedated with a cocktail of tiletamine hydrochloride and zolazepam hydrochloride (Zoletil 100, 8 mg/kg, intramuscular) and pre-medicated with atropine sulfate (0.1 mg/kg, intramuscular). General anaesthesia was subsequently induced with propofol (2–4 mg/kg, intravenous) and maintained with 1–2% isoflurane in 60% air and 40% oxygen. After thoracotomy at the fifth intercostal space, MI was induced by ligating the left anterior descending coronary artery (LAD) below the second diagonal branch.

Ninety minutes later, the pale, ischaemic zone was visually identified, then 1×10^7 FMhMSCs (FMhMSCs group) resuspended in 1 mL of sterile saline solution, or HBR pre-conditioned FMhMSCs (HBR-FMhMSCs group) resuspended in 1 mL of sterile saline solution, or 1 mL of sterile saline solution without HBR (PBS group), was injected intramyocardially through a 21-gauge needle, both in the centre of the infarcted area and along the infarct border (0.1 mL per injection). Owing to early and delayed post-infarct deaths, the protocol could be completed in seven FMhMSCs, six HBR-FMhMSCs and seven PBS group pigs. Sham-operated animals (control group, $n = 4$), in which the LAD was not ligated, were used as normal control animals. This protocol was approved by the Italian Ministry of Health and was in accordance with the Italian law (DL-116, 27 January 1992), which conforms to the *Guide for the Care and Use of Laboratory Animals* published by the US National Institutes of Health (NIH publication no. 85-23, revised 1996; see Supplementary material online).

2.4 *In vivo* imaging

Four weeks after MI, cardiac MRI and PET were performed, and haemodynamic recordings taken to evaluate global and regional changes in myocardial contractility, perfusion, and viability. For non-invasive and invasive diagnostic assessments, the animals were sedated with a continuous infusion of midazolam (0.1 mg kg^{-1} h^{-1} intravenous), allowed to breath spontaneously and positioned lying on their right side with the heart at the isocentre of the gantry unit. It was previously shown that similar doses of midazolam have an irrelevant effect on global and regional cardiac function.[10] Regional LV myocardial perfusion and glucose uptake were measured by PET, whereas LV regional contractility and infarct scar size were assessed by MRI, according to previously standardized protocols.[6] For both imaging techniques, the heart was scanned along basal, middle and apical cross-sectional planes (see Supplementary material online).

2.4.1 MRI measurements

Cine-MRI images were acquired with a 1.5 T scanner (Signa Excite HD; GE Medical Systems, Waukesha, WI, USA), using a non-breath-hold ECG-gated, steady-state free precession pulse sequence (fast imaging employing steady state acquisition).[11] Global (end-diastolic and end-systolic volumes, ejection fraction, and cardiac output) and regional (end-systolic wall thickening, LVWT; and maximal circumferential shortening, $LVEcc_{max}$) LV functional parameters were measured as previously described.[6,12]

To detect and quantify post-infarct myocardial fibrosis, gadolinium-delayed contrast-enhanced (Gd-DE) images were acquired in two-dimensional segmented inversion recovery-prepared gradient echo-sequence, 10 min after administration of contrast agent Gd-DTPA (0.2 mmol/kg intravenous), in short-axis views. In house custom-designed software was used to distinguish the dense infarct core from the heterogeneous infarct periphery ('grey zone'), whose extension is a strong clinical predictor of lethal arrhythmias.[13,14] The endocardial and epicardial borders were outlined on the delayed-enhancement short-axis slices, and then the infarction core and 'grey zone' were quantified as a percentage of the total myocardium.[15]

2.4.2 PET measurements

After overnight fasting, the pigs were scanned in a two-ring positron tomograph ECAT HR Plus (Siemens; CTI, Knoxville, TN, USA). Correct positioning was maintained throughout the study with the aid of a light beam and marks on the pig torso.

Regional myocardial blood flow (MBF) was assessed by [^{13}N]ammonia ($^{13}NH_3$, 10 mCi intravenous bolus). A 10 min transmission scan was obtained to correct for photon attenuation. Acquisition of serial transaxial emission images was started simultaneously with the injection of $^{13}NH_3$. After correction for partial volume effect and recovery coefficient, the image data were computed in a 37 LV segment model using dedicated software (Munich Heart; NM Software, Munich, Germany).

Regional myocardial glucose uptake, an index of myocardial viability, was assessed by ^{18}F-deoxyglucose (^{18}F-FDG, 10 mCi intravenous bolus) followed by an emission scan of 50 min, as previously described.[6]

2.4.3 MRI and PET data analysis

In order to generate complementary data from MRI and PET acquisitions, cardiac images were divided into basal, middle and apical cross-sectional slices, and each slice was divided into 12 segments. The infero-septal border of the infarct area, identified by delayed enhancement, was considered as the reference point, and the segments were counted anticlockwise starting from that point (*Figure 1*). For the sham-operated animals, the reference point was taken as the inferior septum. The segmental data were used to generate 12-point curves corresponding to the following parameters: LV end-systolic wall thickness (LVWT), LV maximal circumferential shortening ($LVEcc_{max}$), and $^{13}NH_3$ and ^{18}F-FDG uptake. The first half of the curve (first six LV segments) was taken to be the area of interest, since it corresponded to the cell-injected myocardium, i.e. infarct and anterior border zone. Uptake of $^{13}NH_3$ and ^{18}F-FDG was calculated in each segment compared with the segment having the highest value of uptake and expressed as the percentage of the maximal uptake. The area under the curve (AUC) of interest was calculated using the trapezoidal rule, as previously described in experimental[16] and clinical studies[17] (*Figure 1*). Data were analysed in blinded fashion under the supervision of cardiologists expert in PET and MRI.

2.5 Haemodynamics

Haemodynamics was assessed in sedated animals 4 weeks after infarction or sham surgery. Arterial pressure was measured via a fluid filled catheter, while LV pressure, dP/dt_{max} and dP/dt_{min} were measured using a solid-state pressure gauge (Millar Instruments Inc., Houston TX, USA) inserted percutaneously through the femoral artery and advanced into the LV cavity under fluoroscopic guidance.[18] The animals were then killed as described in Supplementary material online.

2.6 Histological analysis

Serial sections of 4 μm thickness were used for histological and immunofluorescence analysis. Slices were stained with haematoxylin and eosin or Picro-Mallory trichrome to assess, respectively, tissue structure and extracellular fibrosis. FMhMSCs-derived cells were identified by immunofluorescence using an antibody directed against human mitochondria (anti-Mitochondria, 1:50 dilution, clone 113-1; Millipore, Temecula, CA, USA)[1], and their lineage was determined by co-immunofluorescence identifying specific markers. Cardiac, endothelial, and myofibroblast lineage-committed human cells were detected, respectively, with primary monoclonal antibodies directed against human connexin 43 (Cx43, 1:50 dilution; Invitrogen Corporation, Camarillo, CA, USA), cardiac troponin I (Tn-cI, 1:250 dilution; Abcam, Cambridge, UK), Von Willebrand factor (vWF, 1:2000 dilution; DakoCytomation, Carpenteria, CA, USA), and α-smooth muscle actin (αSMA, 1:9000 dilution; Sigma-Aldrich, MO, USA), which is a reliable marker of myofibroblastic

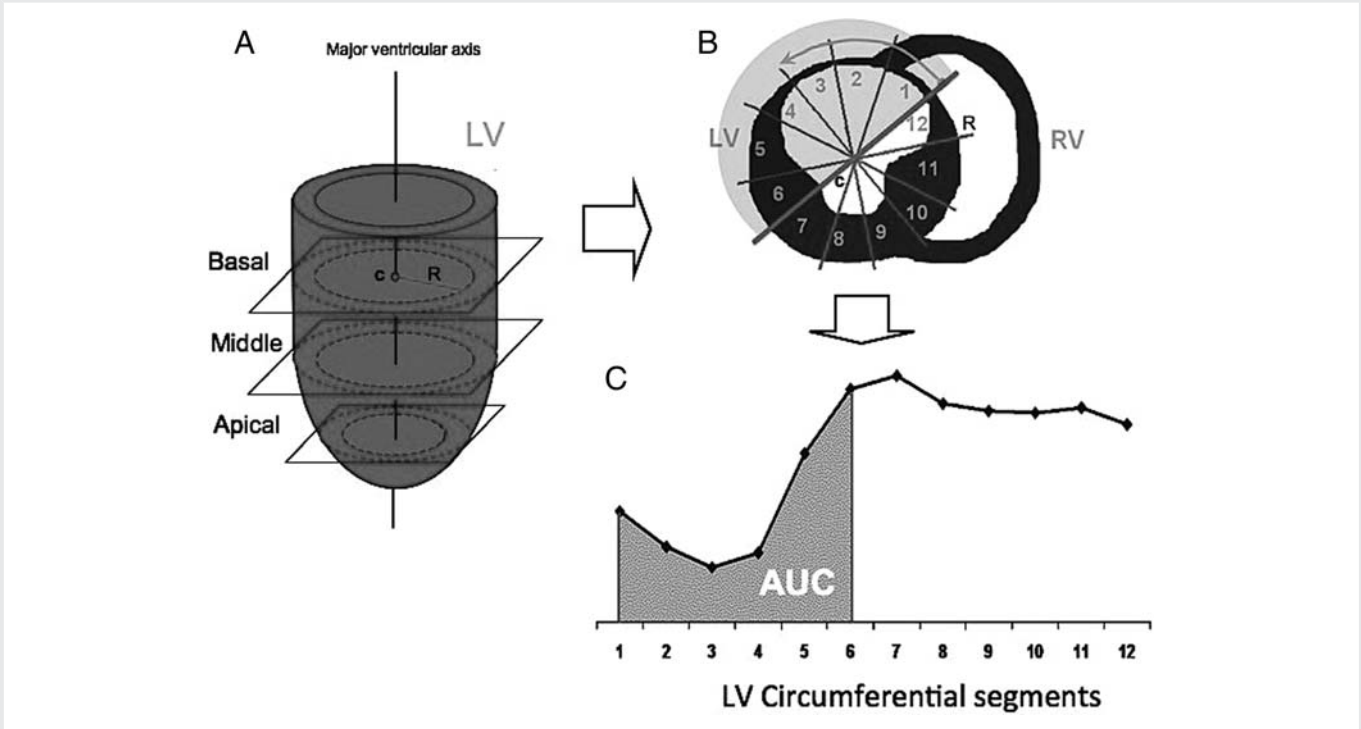

Figure 1 Scheme describing the left ventricle (LV) matched regional analysis with MRI and PET. (*A*) Schematic LV long-axis view and cross-sectional planes (basal, middle, and apical); c, anatomical centroid; and R, LV radius. (*B*) Schematic LV cross-sectional plane in short-axis view and twelve LV circumferential segments; RV, right ventricle; c, anatomical centroid; and R, LV radius. (*C*) Graphical representation of a selected area under curve (AUC).

cells.[19] Endogenous stem cell recruitment was assessed using antibodies directed against Stro-1 (1:100 dilution; R&D Systems, Inc., Minneapolis, MN, USA) and c-kit (1:200 dilution; DakoCytomation, Carpenteria, CA, USA) antigens. Cycling cells were identified with an antibody against the nuclear transcription factor Ki-67 (1:200 dilution; Novocastra Laboratories Ltd, Newcastle, UK; see Supplementary material online).

2.7 Proteomic study

The proteomic profile of LV tissue (5 mg) collected from the infarct border zone was determined in the three infarct groups (PBS, $n = 3$; FMhMSC, $n = 3$; and HBR-FMhMSC, $n = 3$). LV from control animals ($n = 3$) was used as a normal control. The analysis was performed by a multidimensional protein identification technology (MudPIT) approach, as previously described by us and by others (see Supplementary material online).[20,21]

2.8 Statistical analysis

Data are presented as means ± SEM. Statistical analysis was performed by employing commercially available software (SPSS for Windows, version 11.1; SPSS, Chicago, IL, USA). Differences among groups were compared by one- and two-way ANOVA followed by the Bonferroni *post hoc* test. For all the statistical analyses, significance was accepted at $P < 0.05$.

The G-value in proteomic analysis was calculated by employing the method established by Sokal and Rohlf[22] (see Supplementary material online).

3. Results

3.1 Mortality rate and haemodynamics

The overall mortality rate after MI was of 37.5%. The main cause of death was untreatable ventricular arrhythmia following LAD ligation. At 4 weeks, there were no significant differences among groups for heart rate, mean aortic pressure, LV end-diastolic pressure, dP/dt_{max} and dP/dt_{min} (see Supplementary material online, *Table S1*).

3.2 Infarct size determined by MRI

LV total infarct scar size and infarct core zone were not significantly different between the FMhMSCs and PBS groups, but they were reduced by approximately 64 and 44.6%, respectively, in the HBR-FMhMSCs group compared with the other two groups (*Figure 2A* and *B*). In contrast, the grey zone size was not significantly different among the three groups (*Figure 2C*). Representative LV Gd-DE MRI images in short-axis view are showed in *Figure 2D*.

3.3 LV contractile performance

As shown in *Table S1* (see Supplementary material online), 4 weeks after MI the ejection fraction, LV volumes, and cardiac output did not change significantly compared with the control hearts. Nevertheless, the analysis of regional cardiac function revealed marked differences among groups. As shown in *Figure 3A* and *C*, LVWT in segments one to five was depressed in all infarcted groups compared with the sham-operated group; however, it recovered significantly better in segments two and three of the HBR-FMhMSCs group compared with the PBS and FMhMSCs groups. $LVEcc_{max}$, the second index of regional contractile function, also indicated a better recovery in the HBR-FMhMSCs group, although the differences among groups were less pronounced. The overall function of the six LV segments of interest was quantified by AUC, which indeed showed a better recovery of both LVWT and $LVEcc_{max}$ in the HBR-FMhMSCs group compared with the other two infarcted groups (*Figure 3B* and *D*).

3.4 Regional LV perfusion and metabolism

PET-measured myocardial blood perfusion was significantly reduced in LV segments three to five of the FMhMSCs and PBS groups compared with control pigs (*Figure 4A*). In contrast, myocardial perfusion of segments three and four was higher in the HBR-FMhMSCs compared with the PBS and FMhMSCs groups. Consistently, the AUC confirmed that HBR-FMhMSCs was the only group in which the perfusion of the region of interest was significantly higher compared with the PBS group (*Figure 4C*).

As shown in *Figure 4D*, no significant differences could be detected, when considering the single segments, between ^{18}F-FDG uptake in the FMhMSC or HBR-FMhMSC groups vs. the PBS group, and they were all lower than control values. However, when considering the AUC, ^{18}F-FDG uptake was significantly higher in the HBR-FMhMSC, but not in the FMhMSC group, compared with the PBS group (*Figure 4F*).

No significant differences were observed in myocardial perfusion and metabolic rate of glucose of LV remote regions for any experimental conditions.

3.5 Histological analysis

Haematoxylin and eosin tissue staining revealed the presence of a mild inflammatory infiltrate in the LV infarct and border zone with no differences among groups (data not shown). The amount of interstitial collagen in the LV infarct border zone was significantly reduced in the HBR-FMhMSCs group compared with the FMhMSCs and PBS groups (*Figure 2E* and *F*), while no significant changes were observed in the FMhMSCs group compared with the PBS group. As shown in *Figure 2G* and *H*, the density of myocardial capillaries was significantly increased in the LV border zone of the HBR-FMhMSCs group compared with the other infarct groups, whereas angiogenesis was significantly increased in both the FMhMSC and the HBR-FMhMSCs group compared with the PBS group.

Immunofluorescence indicated that the number of human mitochondria-positive cells was significantly higher in the LV border zone of the HBR-FMhMSCs group compared with the other infarct groups (*Figure 5A* and Supplementary material online, *Figure S1A*). To better assess the fate of transplanted human stem cells, we sought specific lineage markers. Double immunofluorescence indicated that the number of human stem cell-derived vessels (*Figure 5B* and Supplementary material online, *Figure S1B*) and αSMA-positive cells in the LV border zone was significantly higher in the HBR-FMhMSCs group compared with the FMhMSCs group (*Figure 5C* and Supplementary material online, *Figure S1C*). In contrast, we could not detect human cells expressing the cardiomyocyte-specific proteins troponin I (*Figure 5D*) and connexin 43, and no markers of endogenously recruited stem cells. A low expression of human Cx43 was expected in αSMA-positive cells[23] derived from transplanted cells, but it is likely that histological analysis was not sufficiently sensitive to detect such small amounts of protein, as previously shown by others.[24] Finally, no cells of human origin were detected in LV of the PBS group or in the remote zones (data not shown). No cells positive for c-kit, Stro-1, and Ki67 were detected in the infarct border zone of any of the groups.

3.6 Proteomic analysis

The hierarchical clustering analysis showed that, overall, the proteomic profile in the LV border zone of the HBR-FMhMSC hearts was

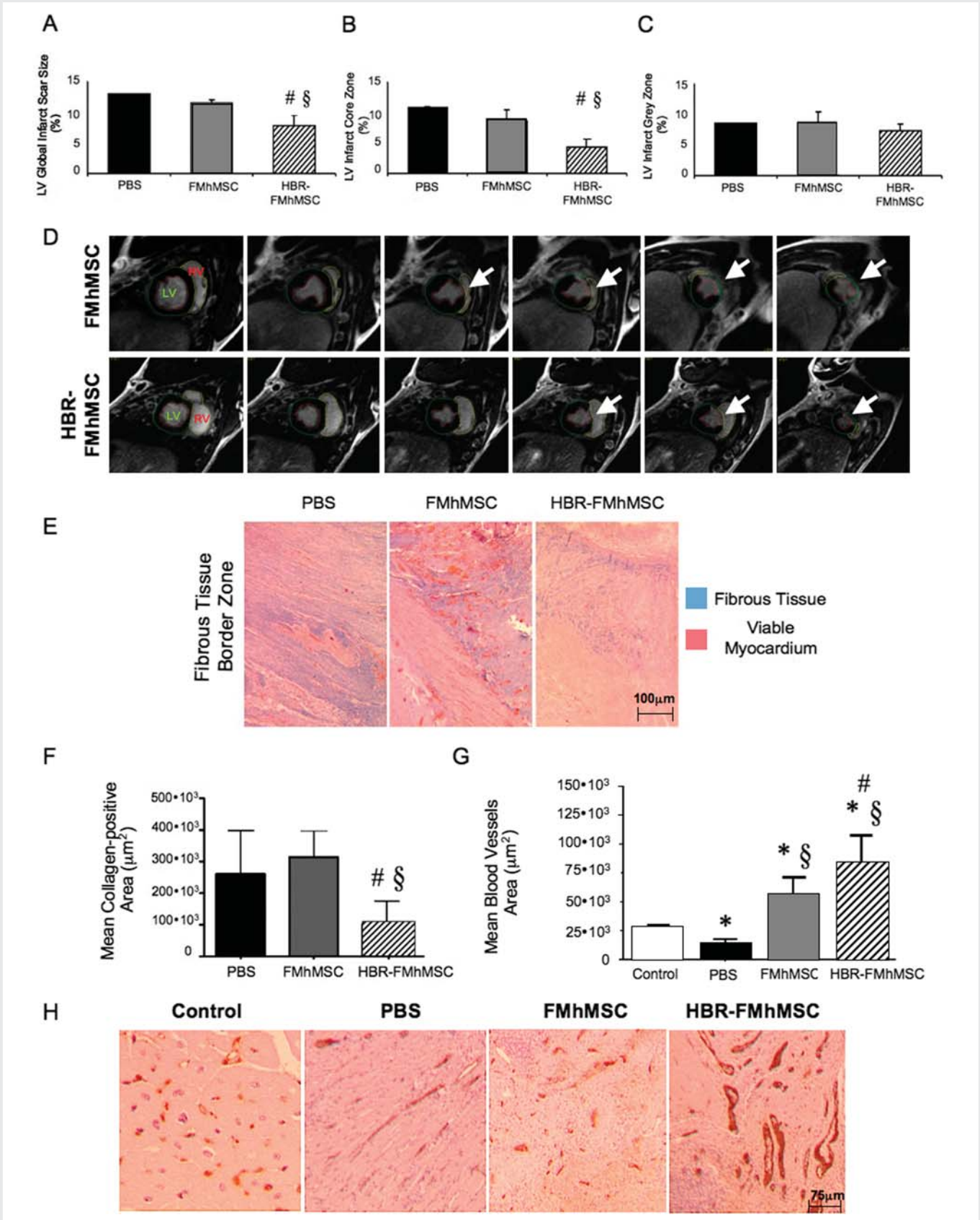

Figure 2 LV infarct size, myocardial fibrosis and angiogenesis. LV global infarct scar size (*A*), core zone (*B*), and grey zone (*C*) measured with Gd-DE MRI as a percentage of total myocardium. (*D*) Representative LV Gd-DE MRI short-axis images. White arrows indicate the LV infarct scar. (*E* and *F*) LV interstitial collagen content in infarct border region. (*G*) LV mean blood vessel area. Values are means + SEM. $^{*}P < 0.05$ vs. control ($n = 4$), $^{\#}P < 0.05$ vs. PBS ($n = 7$), $^{\S}P < 0.05$ vs. FMhMSCs ($n = 7$). (*H*) Immunohistochemical detection of endothelial cells identified by von Willebrand Factor antigen in LV infarct border zone.

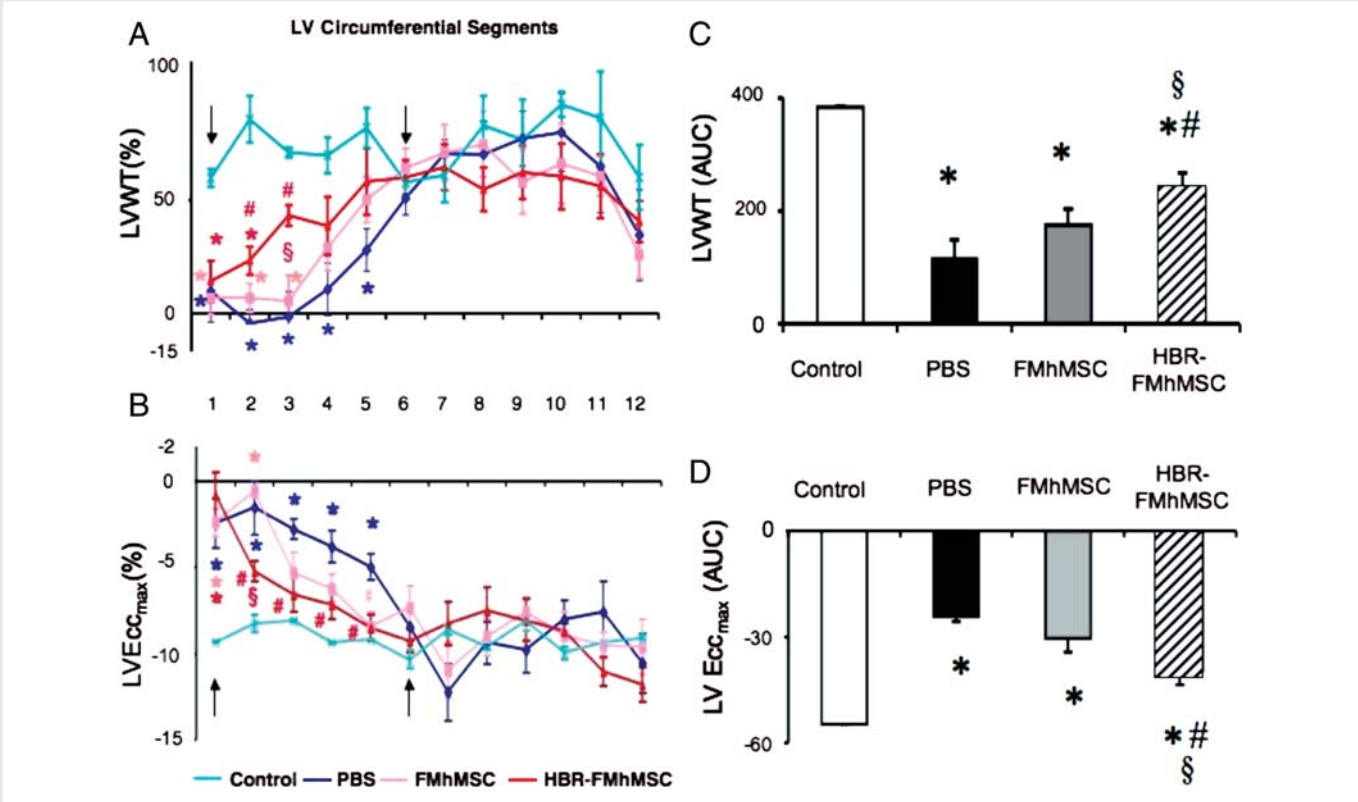

Figure 3 Regional LV contractile function. (*A* and *B*) Segmental LV end-systolic wall thickening (LVWT) and maximal circumferential shortening ($LVEcc_{max}$). Arrows indicate the range of segments considered for measurements of the area under curve (AUC). (*C*) AUC for LVWT. (*D*) Values for AUC for $LVEcc_{max}$. Values are means ± SEM. $^{*}P < 0.05$ vs. control ($n = 4$), $^{\#}P < 0.05$ vs. PBS ($n = 7$), $^{\S}P < 0.05$ vs. FMhMSCs ($n = 7$).

much closer to normal compared with PBS and FMhMSC hearts (*Figure 6A*). In particular, the homology between the protein profile of HBR-FMhMSC hearts and that of normal tissue was 45%, while this homology was 30% for FMhMSC and only 25% for PBS hearts. In contrast, the LV remote zone of all infarcted groups showed a proteomic profile similar to normal. *Figure 6B*, *C* and *D* shows selected metabolic, contractile and pro-survival cardiac proteins that were found to be up- or downregulated in the LV border zone of the three infarcted groups compared with control hearts. In particular, cardiac troponin I, a positive modulator of myocardial contractile function,[25] and carnitine palmitoyltransferase I, the enzyme regulating myocardial mitochondrial fatty acid oxidation,[26] were significantly down-regulated in the PBS group compared with the two groups that received stem cells. Conversely, tenascin C, an extracellular matrix glycoprotein that accelerates adverse ventricular post-infarction remodelling in surviving myocardium,[27] and lumican, a small leucine-rich proteoglycan causing fibrillogenesis in end-stage heart failure,[28] were up-regulated in the PBS group compared with the other two infarcted groups. FMhMSC hearts showed a down-regulation of NADH dehydrogenase and an up-regulation of lumican compared with HBR-FMhMSC hearts.

4. Discussion

The present study shows that placental mesenchymal stem cells pre-treated with HBR display marked reparative capacity in a pig model of acute myocardial infarction. The beneficial effects of this stem cell type have been previously reported by us and by others in rat myocardial infarction[1,3] and are now precisely characterized in a more clinically relevant animal model. Consistent with our previous findings, HBR pre-treatment was critically important to endow placental stem cells with curative potential;[1,29,30] HBR commits mesenchymal stem cells into cardiovascular cell lineages, enhances their secretion of the vasculogenic and pro-trophic factors vascular endothelial growth factor and hepatocyte growth factor (HGF),[1,29] and increases their synthesis of the pro-survival mediators Akt and Pim-1,[29] all effects which might favour their survival, proliferation, and paracrine activity in infarcted hearts.[30]

Other authors have successfully tested mesenchymal stem cells of various origins in infarcted rodents, pigs, and dogs.[31–33] FMhMSCs, first tested by us in rats,[1] have been successfully tested also by others,[3] prompting an editorial on their interesting therapeutic potential.[34] They offer at least two advantages. First, they can be obtained in large amounts from abundant fetal tissue that is otherwise disposed of as biological waste. Second, and more important, it is known that placenta-derived mesenchymal cells do not induce allogeneic or xenogeneic lymphocyte proliferation and actively suppress lymphocyte responsiveness.[35] In fact, similar to rats,[1,3] the fully immunocompetent pigs used in the present study did not activate major immune responses after delivery of FMhMSCs. The absence of tissue rejection in two different animal species subjected to xenotransplantation strongly supports the potential use of FMhMSCs for safe allogeneic cell therapy in humans.

The present findings provide novel information that could have not been obtained without our combined analysis at functional, metabolic,

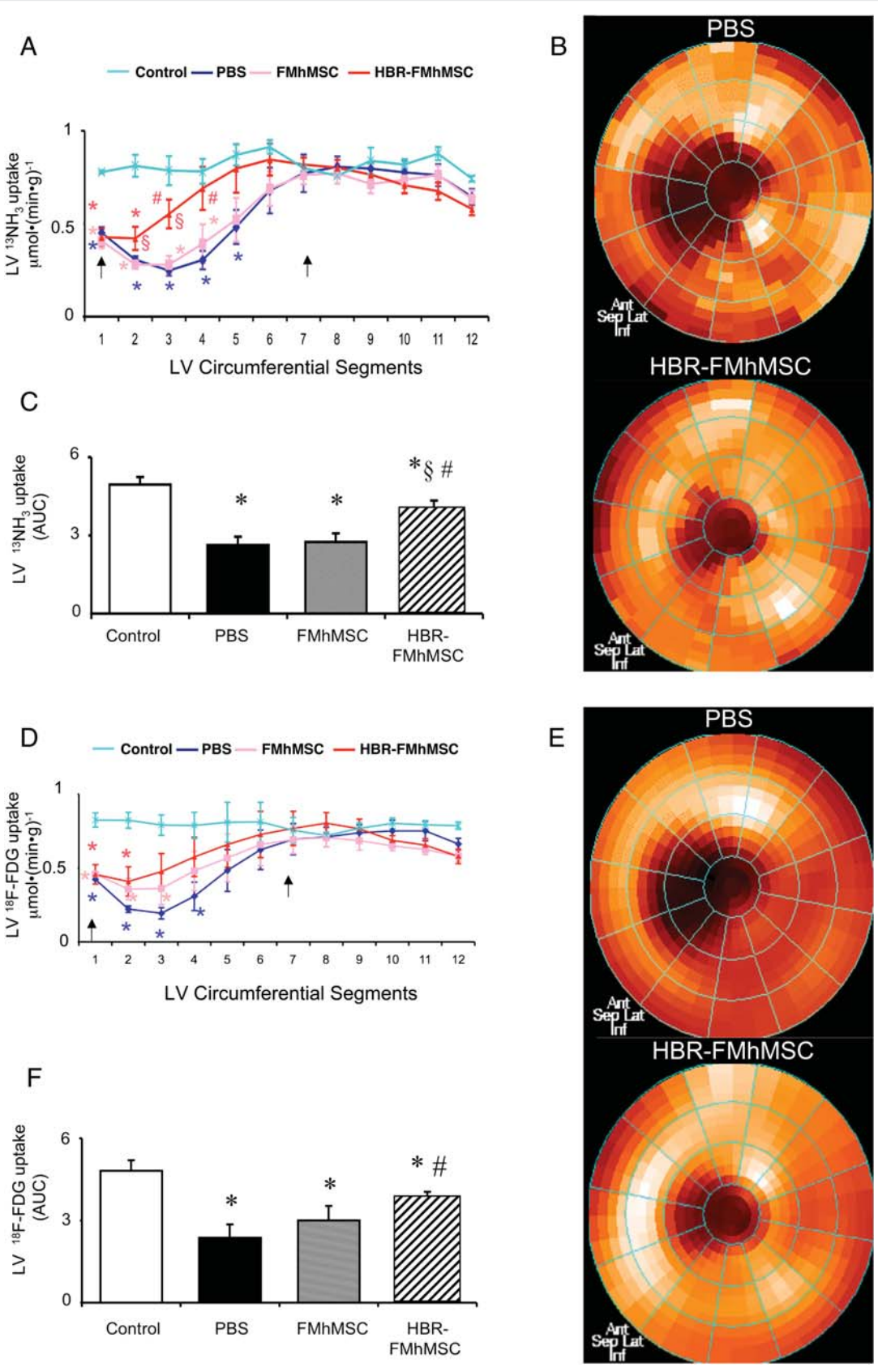

Figure 4 Regional LV myocardial perfusion and myocardial glucose uptake. (*A*) Segmental LV $^{13}NH_3$ myocardial uptake. Black arrows indicate the range of segments considered for measurements of the area under curve (AUC). (*B*) Representative LV bull's eye PET $^{13}NH_3$ images. (*C*) AUC for $^{13}NH_3$ uptake. (*D*) Segmental ^{18}F-FDG myocardial uptake. (*E*) Representative LV bull's eye PET ^{18}F-FDG images. (*F*) AUC for ^{18}F-FDG myocardial uptake. Values are means ± S.E.M. $^{*}P < 0.05$ vs. control ($n = 4$), $^{\#}P < 0.05$ vs. PBS ($n = 7$), $^{\S}P < 0.05$ vs. FMhMSCs ($n = 7$).

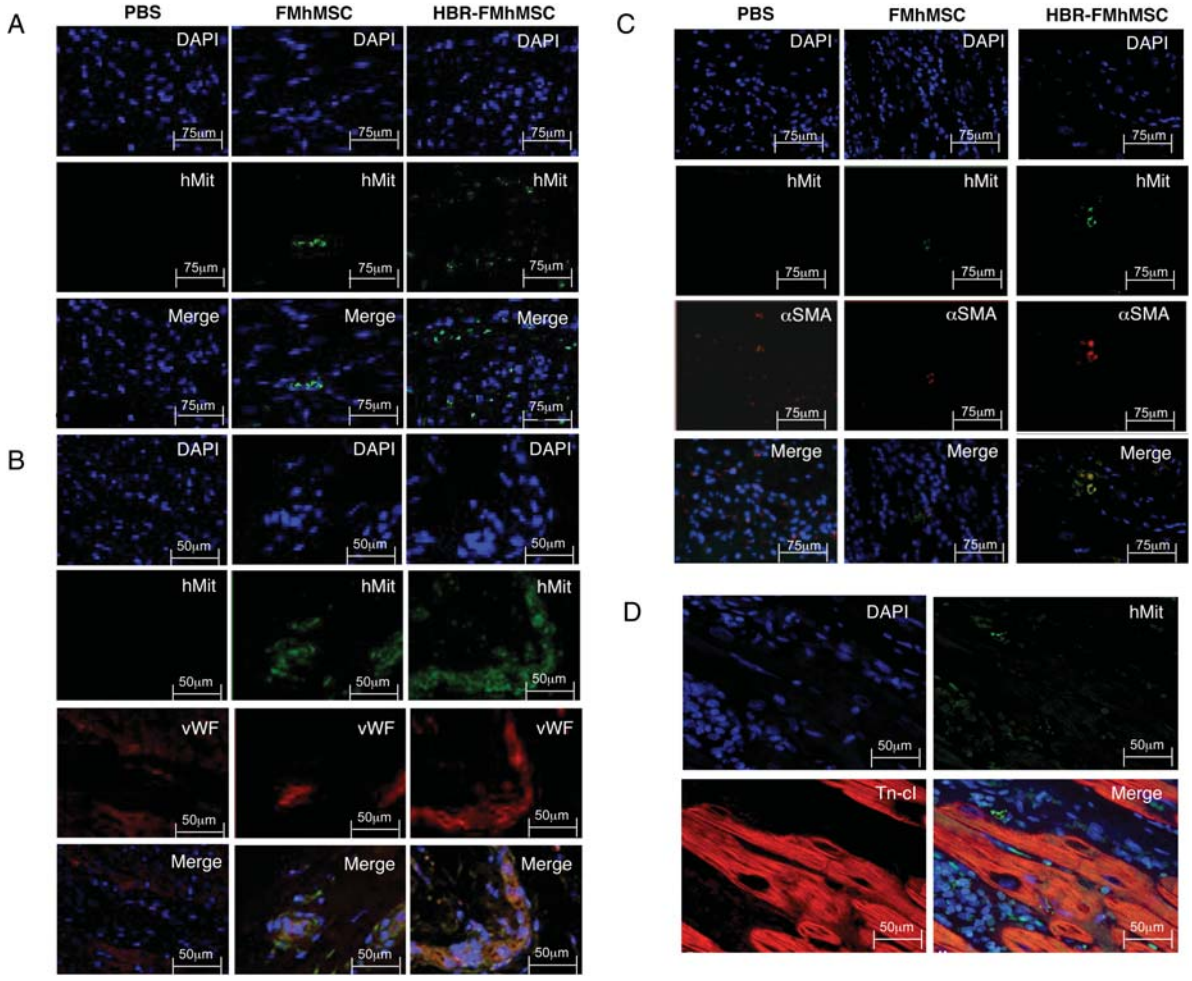

Figure 5 Differentiation of FMhMSCs within the LV infarct border zone. (*A*) Immunofluorescence for human mitochondrial antigen (hMit) for the generic identification of cells of human origin. (*B*) Immunofluorescence for vWF and hMit co-localization to identify FMhMSC-derived vessels. (*C*) Immunofluorescence for αSMA and hMit co-localization to identify FMhMSC-derived myofibroblasts. (*D*) Representative images for Tn-cI and hMit co-localization to identify FMhMSC-derived cells in the HBR-FMhMSC group.

histological, and molecular levels. We established a rigorous and sensitive method, based on state-of-the-art diagnostic imaging, for fine evaluations of regional functional recovery after cell therapy. The size of infarcts induced in our pigs was purposely small to minimize the occurrence of fibrillation or other severe arrhythmias during surgical procedures and/or the acute post-surgical phase. Given the limited extent of cardiac damage, 4 weeks later the haemodynamics and classical parameters of global ventricular function, such as ejection fraction, ventricular volumes, and cardiac output, were not significantly altered compared with sham-operated animals, with no differences among infarcted groups. Our experimental model is consistent with the clinical condition of small myocardial infarction (less than 15%) with preserved global cardiac function, in which no significant correlation is found between infarct size and LV ejection fraction.[36]

MRI delayed enhancement revealed that total infarct size and core were reduced by 64 and 44.6%, respectively, in hearts treated with HBR-FMhMSCs compared with control infarcts. In addition, MRI-aided analysis of cardiac regional function showed significantly improved systolic wall thickening and shortening in hearts treated with HBR-FMhMSCs, especially in those wall segments corresponding to the infarct border zone. PET imaging proved perfectly complementary, as it showed a good match between contractile function and myocardial perfusion in the same ventricular segments. The overall ^{18}F-FDG uptake of the area of interest was also significantly higher in HBR-FMhMSCs-treated relative to untreated infarcts, although this metabolic index revealed less pronounced differences when single segments were compared. Taken together, the information obtained from *in vivo* imaging clearly indicated that delivery of FMhMSCs did not affect the post-infarction outcome, while a significant reduction in infarct size and recovery of cardiac function, perfusion and metabolism was found in animals receiving HBR-FMhMSCs. Again, such quantifiable differences among groups could have not been detected and *in vivo* findings not correctly interpreted without the 'magnifying glass' of MRI/PET assessment of selected cardiac regions.

Histological and proteomic analysis confirmed, *in vitro*, the reliability of *in vivo* cardiac imaging, while, in turn, the *in vivo* cardiac imaging oriented the pathophysiological interpretation of histological changes. As expected, the infarct border zone contained less fibrous tissue in hearts that received HBR-FMhMSCs compared with

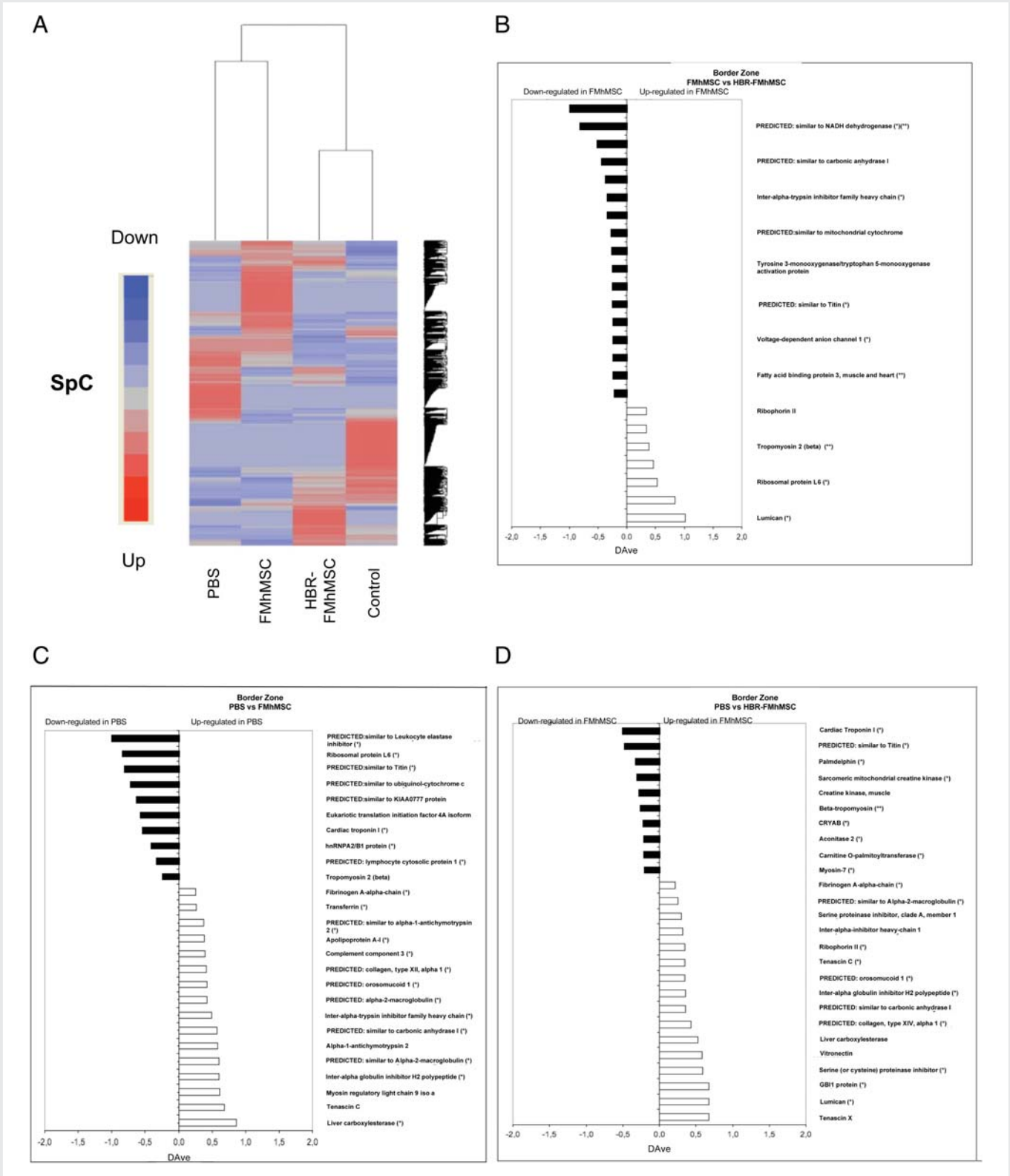

Figure 6 Proteomic profile of the infarct border zone compared with normal myocardium. (*A*) Hierarchical clustering of proteins using the centroid distance method. SpC, spectral counts. (*B*, *C* and *D*) Semiquantitative analysis, in which the bars represent the score ratio expressed by the DAve index. $n = 3$ animals per group. $^*P < 0.05$.

the other two infarcted groups. This seems inconsistent with the absence of significant changes in the grey zone size as detected by MRI. It should be noted, however, that the grey zone corresponds to a very heterogeneous tissue bordering the infarct periphery and is characterized by a mixture of normal and fibrotic myocardium. MRI can provide an estimate of the extension of this area, but cannot be as detailed as the histological analysis in the quantification of fibrotic vs. myocardial tissue. In contrast, albeit more pronounced in hearts injected with HBR-FMhMSCs, microvessel density was higher in both groups of treated hearts compared with control infarcts. In this case, the *in vivo* analysis proved necessary to avoid misinterpretations based on histology. In fact, despite significant vascular regeneration, border zone blood perfusion in hearts injected with FMhMSCs did not recover compared with control infarcts. Interestingly, the transplanted human stem cells seemed to differentiate only as endothelial and smooth muscle cells, thus directly contributing to vessel, but not to cardiomyocyte, regeneration. This finding is in contrast with our previous data in rats,[1] and supports the concept that, after cardiac delivery, stem cells take only little part in direct tissue regeneration, for instance by forming new vessels, while they might exert protective or pro-regenerative effects on surviving cardiomyocytes and other cell types by releasing paracrine factors.[29,37] These include vascular endothelial growth factor, fibroblast growth factor-2, and HGF genes and enhanced secretion of their related products. It is conceivable that the pro-regenerative effects of conditioned stem cells are due to the enhancement of their paracrine activity, as suggested by our recent study in infarcted rat hearts injected with pure HBR.[29]

Proteomic analysis is a formidable tool of investigation that, to date, has been little exploited for studies of cardiac cell therapy and might prove even more powerful if combined with *in vivo* imaging.[38] A clear advantage offered by overall protein expression profiling is the possibility to determine the phenotype of damaged and regenerating tissue, thus identifying differences that might suggest key molecular mechanisms involved in the reparative process, and to compare it with normal tissue in order to assess the biological effects of specific stem cell types. In the present study, proteomic analysis nicely corroborated *in vivo* findings, indicating a 45% homology between protein expressions in the border zone of hearts treated with HBR-FMhMSCs and normal tissue. Less homology was found in hearts receiving FMhMSCs, consistent with the smaller functional recovery favoured by those cells, despite their pro-angiogenic effect. Among the many alterations in protein expression that emerged from our analysis and that deserve future *ad hoc* studies, it is noteworthy that lumican, a member of the small leucine-rich proteoglycan family, was up-regulated in the border zone of hearts treated with FMhMSC, but not HBR-FMhMSC. Lumican contributes mainly to collagen fibre assembly and organization in fibrotic tissue of ischaemic myocardium and is localized in fibrotic tissue.[28,39] Moreover, the reduced expression of critically important mitochondrial enzymes, such as NADH dehydrogenase and/or cytochrome complexes, points to an impaired metabolism in the border zone in the FMhMSCs and PBS groups, in accord with the reduced ^{18}F-FDG uptake assessed by PET. The fatty acid binding protein, necessary for the facilitated transport of fatty acid into cardiomyocytes, was also decreased; notoriously, fatty acids are the main cardiac energy substrate.[40] It is also interesting that carbonic anhydrase I, an intracellular pH sensor which plays an important role in the cardiac cell response to ischaemic acidosis,[41] was downregulated in hearts treated with FMhMSCs. Unfortunately, the 'omic' approach is not designed to test mechanisms; therefore, we do not know whether enzymatic changes were causally related to biochemical or to functional alterations, or both. In any case, they were not observed in infarcted hearts treated with HBR-FMhMSC, suggesting a better post-infarct recovery of the metabolic phenotype.

An important limitation of our study is the use of small infarcts, with no changes in ejection fraction, to test the regional effects of stem cell therapy. This was very convenient to obtain a consistent experimental preparation and reduce pig mortality; however, further studies will be necessary to test whether HBR pre-treatment can potentiate mesenchymal stem cell therapy in a large-animal model of myocardial infarction with global depression of cardiac function.

In conclusion, our study defined, in a clinically relevant animal model, the beneficial effects of placental mesenchymal stem cells delivered to infarcted hearts and the need for their *ex vivo* preconditioning with molecules harbouring differentiating and paracrine 'logics' before transplantation. Our investigation provides new information generated by a novel multimodal *in vivo* and *in vitro* analysis. This dual imaging should be recommended at least for pilot assessments of cardiac therapy with new stem cell candidates, so as to avoid underestimations due to the use of indices such as ejection fraction and systemic haemodynamics, which may not be sufficiently sensitive.

Supplementary material

Supplementary material is available at *Cardiovascular Research* online.

Acknowledgements

We are grateful to Drs Silvia Burchielli and Elena Olivi for their excellent technical assistance.

Conflict of interest: none declared.

Funding

This work was supported by Compagnia di San Paolo, Torino, Italy (F.A.R.), and in part by Regione Emilia Romagna, Programma di Ricerca Regione-Università 2007/2009, Area 1b 'Medicina Rigenerativa' Bologna, Italy (C.V.), and intramural funds of the Institute of Clinical Physiology, CNR-Fondazione G. Monasterio, Pisa, Italy (F.A.R.). F.A.R. is an Established Investigator of the American Heart Association.

References

1. Ventura C, Cantoni S, Bianchi F, Lionetti V, Cavallini C, Scarlata I *et al.* Hyaluronan mixed esters of butyric and retinoic acid drive cardiac and endothelial fate in term placenta human mesenchymal stem cells and enhance cardiac repair in infarcted rat hearts. *J Biol Chem* 2007;**282**:14243–14252.
2. Parolini O, Alviano F, Bagnara GP, Bilic G, Bühring HJ, Evangelista M *et al.* Concise review: isolation and characterization of cells from human term placenta: outcome of the first international Workshop on Placenta Derived Stem Cells. *Stem Cells* 2008;**26**:300–311.
3. Tsuji H, Miyoshi S, Ikegami Y, Hida N, Asada H, Togashi I *et al.* Xenografted human amniotic membrane-derived mesenchymal stem cells are immunologically tolerated and transdifferentiated into cardiomyocytes. *Circ Res* 2010;**106**:1613–1623.
4. Barlow S, Brooke G, Chatterjee K, Price G, Pelekanos R, Rossetti T *et al.* Comparison of human placenta- and bone marrow-derived multipotent mesenchymal stem cells. *Stem Cells Dev* 2008;**17**:1095–1107.
5. Wu KC, Lima JA. Noninvasive imaging of myocardial viability: current techniques and future developments. *Circ Res* 2003;**93**:1146–1158.
6. Lionetti V, Guiducci L, Simioniuc A, Aquaro GD, Simi C, De Marchi D *et al.* Mismatch between uniform increase in cardiac glucose uptake and regional contractile dysfunction in pacing-induced heart failure. *Am J Physiol Heart Circ Physiol* 2007;**293**:H2747–H2756.

7. Masci PG, Ganame J, Strata E, Desmet W, Aquaro GD, Dymarkowski S *et al*. Myocardial salvage by CMR correlates with LV remodeling and early ST-segment resolution in acute myocardial infarction. *JACC Cardiovasc Imaging* 2010;**3**:45–51.
8. Amado LC, Schuleri KH, Saliaris AP, Boyle AJ, Helm R, Oskouei B *et al*. Multimodality noninvasive imaging demonstrates in vivo cardiac regeneration after mesenchymal stem cell therapy. *J Am Coll Cardiol* 2006;**48**:2116–2124.
9. Ventura C, Maioli M, Asara Y, Santoni D, Scarlata I, Cantoni S *et al*. Butyric and retinoic mixed ester of hyaluronan. A novel differentiating glycoconjugate affording a high throughput of cardiogenesis in embryonic stem cells. *J Biol Chem* 2004;**279**: 23574–23579.
10. Smith AC, Zellner JL, Spinale FG, Swindle MM. Sedative and cardiovascular effects of midazolam in swine. *Lab Anim Sci* 1991;**41**:157–161.
11. Slavin GS, Saranathan M. FIESTA-ET: high-resolution cardiac imaging using echo-planar steady-state free precession. *Magn Reson Med* 2002;**48**:934–941.
12. Lionetti V, Aquaro GD, Simioniuc A, Di Cristofano C, Forini F, Cecchetti F *et al*. Severe mechanical dyssynchrony causes regional hibernation-like changes in pigs with nonischemic heart failure. *J Card Fail* 2009;**15**:920–928.
13. Roes SD, Borleffs CJ, van der Geest RJ, Westenberg JJ, Marsan NA, Kaandorp TA *et al*. Infarct tissue heterogeneity assessed with contrast-enhanced MRI predicts spontaneous ventricular arrhythmia in patients with ischemic cardiomyopathy and implantable cardioverter-defibrillator. *Circ Cardiovasc Imaging* 2009;**2**:183–190.
14. Schmidt A, Azevedo CF, Cheng A, Gupta SN, Bluemke DA, Foo TK *et al*. Infarct tissue heterogeneity by magnetic resonance imaging identifies enhanced cardiac arrhythmia susceptibility in patients with left ventricular dysfunction. *Circulation* 2007;**115**: 2006–2014.
15. Yan AT, Shayne AJ, Brown KA, Gupta SN, Chan CW, Luu TM *et al*. Characterization of the peri-infarct zone by contrast-enhanced cardiac magnetic resonance imaging is a powerful predictor of post-myocardial infarction mortality. *Circulation* 2006;**114**: 32–39.
16. Fang YH, Muzic RF Jr. Spillover and partial-volume correction for image-derived input functions for small-animal ^{18}F-FDG PET studies. *J Nucl Med* 2008;**49**:606–614.
17. Koch KC, vom Dahl J, Wenderdel M, Nowak B, Schaefer WM, Sasse A *et al*. Myocardial viability assessment by endocardial electroanatomic mapping: comparison with metabolic imaging and functional recovery after coronary revascularization. *J Am Coll Cardiol* 2001;**38**:91–98.
18. Gemignani V, Bianchini E, Faita F, Lionetti V, Campan M, Recchia FA *et al*. Transthoracic sensor for noninvasive assessment of left ventricular contractility: validation in a minipig model of chronic heart failure. *Pacing Clin Electrophysiol* 2010;**33**:795–803.
19. Willems IE, Havenith MG, De Mey JG, Daemen MJ. The α-smooth muscle actin-positive cells in healing human myocardial scars. *Am J Pathol* 1994;**145**:868–875.
20. Mauri P, Scarpa A, Nascimbeni AC, Benazzi L, Parmagnani E, Mafficini A *et al*. Identification of proteins released by pancreatic cancer cells by multidimensional protein identification technology: a strategy for identification of novel cancer markers. *FASEB J* 2005;**19**:1125–1127.
21. Kislinger T, Gramolini AO, MacLennan DH, Emili A. Multidimensional protein identification technology (MudPIT): technical overview of a profiling method optimized for the comprehensive proteomic investigation of normal and diseased heart tissue. *J Am Soc Mass Spectrom* 2005;**16**:1207–1220.
22. Sokal RR, Rohlf FJ. *Biometry: the Principles and Practice of Statistics in Biological Research*, 3rd edn. New York: Freeman, 1994.
23. Roell W, Lewalter T, Sasse P, Tallini YN, Choi BR, Breitbach M *et al*. Engraftment of connexin 43-expressing cells prevents post-infarct arrhythmia. *Nature* 2007;**450**: 819–824.
24. Zhang Y, Kanter EM, Laing JG, Aprhys C, Johns DC, Kardami E *et al*. Connexin43 expression levels influence intercellular coupling and cell proliferation of native murine cardiac fibroblasts. *Cell Commun Adhes* 2008;**15**:289–303.
25. Palmer BM. Thick filament proteins and performance in human heart failure. *Heart Fail Rev* 2005;**10**:187–197.
26. Lionetti V, Linke A, Chandler MP, Young ME, Penn MS, Gupte S *et al*. Carnitine palmitoyl transferase-I inhibition prevents ventricular remodeling and delays decompensation in pacing-induced heart failure. *Cardiovasc Res* 2005;**66**:454–461.
27. Nishioka T, Onishi K, Shimojo N, Nagano Y, Matsusaka H, Ikeuchi M *et al*. Tenascin-C may aggravate left ventricular remodeling and function after myocardial infarction in mice. *Am J Physiol Heart Circ Physiol* 2010;**298**:H1072–H1078.
28. Hwang JJ, Allen PD, Tseng GC, Lam CW, Fananapazir L, Dzau VJ *et al*. Microarray gene expression profiles in dilated and hypertrophic cardiomyopathic end-stage heart failure. *Physiol Genomics* 2002;**10**:31–44.
29. Lionetti V, Cantoni S, Cavallini C, Bianchi F, Valente S, Frascari I *et al*. Hyaluronan mixed esters of butyric and retinoic acid affording myocardial survival and repair without stem cell transplantation. *J Biol Chem* 2010;**285**:9949–9961.
30. Gnecchi M, Zhang Z, Ni A, Dzau VJ. Paracrine mechanisms in adult stem cell signaling and therapy. *Circ Res* 2008;**103**:1204–1219.
31. Dai W, Hale SL, Martin BJ, Kuang JQ, Dow JS, Wold LE *et al*. Allogeneic mesenchymal stem cell transplantation in postinfarcted rat myocardium: short- and long-term effects. *Circulation* 2005;**112**:214–223.
32. Wolf D, Reinhard A, Seckinger A, Katus HA, Kuecherer H, Hansen A. Dose-dependent effects of intravenous allogeneic mesenchymal stem cells in the infarcted porcine heart. *Stem Cells Dev* 2009;**18**:321–329.
33. Silva GV, Litovsky S, Assad JA, Sousa AL, Martin BJ, Vela D *et al*. Mesenchymal stem cells differentiate into an endothelial phenotype, enhance vascular density, and improve heart function in a canine chronic ischemia model. *Circulation* 2005;**111**: 150–156.
34. Penn MS, Mayorga ME. Searching for understanding with the cellular lining of life. *Circ Res* 2010;**106**:1554–1556.
35. Chang CJ, Yen ML, Chen YC, Chien CC, Huang HI, Bai CH *et al*. Placenta-derived multipotent cells exhibit immunosuppressive properties that are enhanced in the presence of interferon-γ. *Stem Cells* 2006;**24**:2466–2477.
36. Pride YB, Giuseffi JL, Mohanavelu S, Harrigan CJ, Manning WJ, Gibson CM *et al*. Relation between infarct size in ST-segment elevation myocardial infarction treated successfully by percutaneous coronary intervention and left ventricular ejection fraction three months after the infarct. *Am J Cardiol* 2010;**106**:635–640.
37. Chimenti I, Smith RR, Li TS, Gerstenblith G, Messina E, Giacomello A *et al*. Relative roles of direct regeneration versus paracrine effects of human cardiosphere-derived cells transplanted into infarcted mice. *Circ Res* 2010;**106**:971–980.
38. Chun HJ, Wilson KO, Huang M, Wu JC. Integration of genomics, proteomics, and imaging for cardiac stem cell therapy. *Eur J Nucl Med Mol Imaging* 2007;**34**(Suppl. 1):S20–S26.
39. Baba H, Ishiwata T, Takashi E, Xu G, Asano G. Expression and localization of lumican in the ischemic and reperfused rat heart. *Jpn Circ J* 2001;**65**:445–450.
40. Lopaschuk GD, Ussher JR, Folmes CD, Jaswal JS, Stanley WC. Myocardial fatty acid metabolism in health and disease. *Physiol Rev* 2010;**90**:207–258.
41. Vandenberg JI, Carter ND, Bethell HW, Nogradi A, Ridderstråle Y, Metcalfe JC *et al*. Carbonic anhydrase and cardiac pH regulation. *Am J Physiol* 1996;**271**: C1838–C1846.